Astron. Astrophys. 358, 612–616 (2000)

ASTRONOMY AND ASTROPHYSICS

Accretion disk structure of adiabatic and magnetised CTTS-systems

D. Elstner and G. Rüdiger

Astrophysikalisches Institut Potsdam, An der Sternwarte 16, 14482 Potsdam, Germany

Received 10 March 2000 / Accepted 7 April 2000

Abstract. The role of a large-scale magnetic field in a classical TTS star-disk system is studied. The central object yields a magnetic dipolar field which is modified and amplified by the accretion disk. The entropy in the equatorial plane is assumed as unchanged by the magnetic field. The disk halo is considered as a plasma with the same conductivity as the disk and corotating with the star. The induced toroidal fields are confirming a former estimate by Campbell (1992); their (vertical) angular momentum transport strictly changes the accretion disk structure. For rather weak magnetic fields there is no disk inside the corotation radius, but outside the corotation radius the disk becomes much warmer, thicker and more massive than the corresponding non-magnetic solutions. For stellar magnetic field exceeding 2000 Gauss we find the maximal magnetic torque starting to saturate.

Key words: accretion, accretion disks – Magnetohydrodynamics (MHD) – stars: formation

1. Motivation

Young stellar objects (YSO) are formed by 3 main components: (a) a protostar, (b) an accretion disk and (c) bipolar outflows which all are connected by a large-scale magnetic field (Fendt & Camenzind 1996). Radio observations suggest the existence of a magnetic field of order of kGauss on the surface of the protostar (André et al. 1991).

The interaction between the gaseous and the electromagnetic components of the system is certainly complex. The magnetic field will thread the accretion disk to change its structure and the accretion-disk flow pattern will change the field geometry. The latter is known as the ‘field dragging’ happening beyond the disk surfaces (Ghosh & Lamb 1979; Königl 1991; Lubow et al. 1994; Reyes-Ruiz & Stepinski 1996; Shalybkov & Rüdiger 2000). The differential rotation in the system can deform the magnetic field in a way that hydromagnetic jet structures are formed (Blandford & Payne 1982; Pudritz 1983; Königl 1989).

Ogilvie (1997) and Ogilvie & Livio (1998) study the vertical structure of a disk under the influence of the Maxwell stress for vanishing toroidal fields. The magnetic pressure becomes so strong that the rotation law becomes non-Keplerian and the jet launching is complicated. Livio & Pringle (1992) focus to the radial structure of the magnetised disk embedded in a dipolar stellar field. The strong *vertical* gradient of the angular velocity between disk and halo forms a strong toroidal field at the disk-halo surface which i) changes the accretion disk structure, ii) transports angular momentum and iii) produces Joule heat. In particular the latter effect seems to avoid the existence of stationary solutions due to an enhanced influence of the radiation pressure in the inner part of the disk (Brandenburg & Campbell 1998).

In the present paper only one isolated aspect of the full interplay is considered, i.e. the influence of a given stellar (or interstellar) field on the structure of the accretion disk. In the standard-accretion disk theory the material is assumed as a high-viscosity fluid in order to transfer a big amount of angular momentum. The viscosity can (only) be imagined as due to the action of intensive turbulence. If this is true the material should also possess a high magnetic diffusivity the relation of which to the viscosity is given by the magnetic Prandtl number Pm. The nonuniform Keplerian rotation induces toroidal magnetic belts in the accretion disk with consequences for its structure. The magnitude of the field follows from the adopted turbulence parameters which can be tested for consistency along this way.

2. Basic equations

2.1. Magnetic field

We assume the magnetic field of the central star as an external dipole hence, if the field is undisturbed by the disk,

$$\boldsymbol{B}^{(0)} = \begin{pmatrix} 3\cos\theta\sin\theta \\ 0 \\ 3\cos^2\theta - 1 \end{pmatrix} \left(\frac{R_*}{r}\right)^3 \hat{B} \tag{1}$$

in cylindrical coordinates (R, ϕ, Z), θ is the colatitude and r the radial distance. In the equatorial plane we have only a Z-component of the field, i.e.

$$B_Z^0 = -\left(\frac{R_*}{R}\right)^3 \hat{B} \tag{2}$$

Send offprint requests to: D. Elstner (delstner@aip.de)

with $\hat{B}$ as the magnetic field amplitude on the stellar surface $R = R_*$.

The accretion disk forms a fluid with laminar and random velocity field, $\boldsymbol{u} = \bar{\boldsymbol{u}} + \boldsymbol{u}'$. Both contributions to the flow pattern are modifying the magnetic field so that it makes sense to write $\bar{\boldsymbol{B}} = \boldsymbol{B}^{(0)} + \tilde{\boldsymbol{B}}$, where $\tilde{\boldsymbol{B}}$ is the disk-flow induced part of the magnetic field.

The evolution of the mean magnetic field $\bar{\boldsymbol{B}}$ is governed by the induction equation

$$\frac{\partial \bar{\boldsymbol{B}}}{\partial t} = \mathrm{rot}\,(\bar{\boldsymbol{u}} \times \bar{\boldsymbol{B}} + \boldsymbol{\mathcal{E}}), \qquad (3)$$

where $\boldsymbol{\mathcal{E}}$ is the turbulent electromotive force, $\boldsymbol{\mathcal{E}} = \langle \boldsymbol{u}' \times \boldsymbol{B}' \rangle$, and $\bar{\boldsymbol{u}}$ the mean velocity. The molecular magnetic diffusivity is negligible in comparison with the turbulent diffusion.

We assume approximate scale-separation and write $\mathcal{E}_i = \eta_{ijk}\bar{B}_{j,k} + ...$ The turbulent magnetic diffusivity tensor exists even without basic rotation. In the absence of any anisotropies it is simply $\eta_{ijk} = \eta_{\mathrm{T}}\epsilon_{ijk}$ so that $\boldsymbol{\mathcal{E}} = -\eta_{\mathrm{T}}\,\mathrm{rot}\,\bar{\boldsymbol{B}}$. The eddy diffusivity, however, is only a simple tensor unless the magnetic field feeds back. Then the η-tensor becomes much more complex, i.e. $\eta_{ijk} = \eta_{\mathrm{T}}(\bar{B})\,\epsilon_{ijk} + \hat{\eta}(\bar{B})\,\epsilon_{ilk}\bar{B}_j\bar{B}_l + ...$

The reference value for the eddy diffusivity is

$$\eta_0 = \nu_0/\mathrm{Pm}, \qquad (4)$$

taken for diffusivities for vanishing magnetic field. We shall work here with the traditional value of Pm = 1.

As the external magnetic dipole is steady and current-free (3) changes to

$$\frac{\partial \tilde{\boldsymbol{B}}}{\partial t} - \mathrm{rot}\left(\bar{\boldsymbol{u}} \times \tilde{\boldsymbol{B}} - \eta_{\mathrm{T}}\,\mathrm{rot}\,\tilde{\boldsymbol{B}}\right) = \mathrm{rot}\left(\bar{\boldsymbol{u}} \times \boldsymbol{B}^{(0)}\right), \qquad (5)$$

wherein the RHS of this equation acts in the sense of a source term.

2.2. Disk equations

In Livio & Pringle (1992) a toroidal field is induced by the *vertical* gradient of the angular velocity computed in the system corotating with the star. The magnetic pressure formed by the toroidal field acts in vertical as well as radial direction with consequences for the thickness and the rotation law of the disk. Additionally, there is an angular momentum transport by the Maxwell stress which may easily act as a driver of the overall inward accretion flow. These terms are derived in the following.

In cylindric coordinates the conservation law of mass reads

$$\frac{\partial \rho}{\partial t} + \frac{1}{R}\frac{\partial}{\partial R}(R\rho\bar{u}_R) + \frac{\partial}{\partial Z}(\rho\bar{u}_Z) = 0. \qquad (6)$$

After an integration over Z is

$$\frac{\partial \Sigma}{\partial t} + \frac{1}{R}\frac{\partial}{\partial R}\big(R\Sigma\bar{u}_R\big) = 0 \qquad (7)$$

or $2\pi R\Sigma\bar{u}_R = -\dot{M}$ with

$$\Sigma = \int_{-\infty}^{\infty} \rho dZ \qquad (8)$$

in the stationary case. The magnetic field appears in the momentum equation. Its radial part provides

$$\rho\,\frac{\partial \bar{u}_R}{\partial t} + \rho\bar{u}_R\frac{\partial \bar{u}_R}{\partial R} + \frac{\partial p}{\partial R} + \frac{1}{3}\frac{\partial}{\partial R}\big(\rho\langle \boldsymbol{u}'^2\rangle\big) - \rho R\Omega^2 = = -GM\frac{\rho}{R^2} - \frac{1}{2\mu_0 R^2}\frac{\partial}{\partial R}\left(R^2\bar{B}_\phi^2\right) \qquad (9)$$

if – as assumed – the toroidal fields dominate. Here M is the central mass and p the gas pressure. If all terms could be neglected except centrifugal force and central gravitation, the Kepler law $\Omega_{\mathrm{K}} = \sqrt{GM/R^3}$ results. Integration of (9) over Z yields

$$\Sigma\,\frac{\partial \bar{u}_R}{\partial t} + \Sigma\bar{u}_R\frac{\partial \bar{u}_R}{\partial R} + \frac{\partial \Pi}{\partial R} + + \frac{1}{3}\frac{\partial}{\partial R}\big(\Sigma\langle \boldsymbol{u}'^2\rangle\big) = \left(-\frac{GM}{R^2} + R\Omega^2\right)\Sigma + \mathcal{B}_R \qquad (10)$$

with

$$\Pi = \int_{-\infty}^{\infty} p\,dZ \qquad (11)$$

and

$$\mathcal{B}_R = -\frac{1}{2\mu_0 R^2}\frac{d}{dR}\int_{-\infty}^{\infty} R^2\bar{B}_\phi^2\,dZ. \qquad (12)$$

We only use the RHS of (10) and write

$$\left(-\frac{GM}{R^2} + R\Omega^2\right)\Sigma + \mathcal{B}_R = 0. \qquad (13)$$

The conservation law of angular momentum is the ϕ-component of the Reynolds equation,

$$\frac{\partial}{\partial t}(\rho R^2\Omega) + \mathrm{div}\,\boldsymbol{t} = 0, \qquad (14)$$

with

$$\boldsymbol{t} = \rho R^2\Omega\bar{\boldsymbol{u}} + \rho R\langle u_\phi'\boldsymbol{u}'\rangle - \frac{R}{\mu_0}\bar{B}_\phi\bar{\boldsymbol{B}}. \qquad (15)$$

As usual the basic stress-strain relation

$$\langle u_i'u_j'\rangle = \frac{1}{3}\langle \boldsymbol{u}'^2\rangle\delta_{ij} - \nu_{\mathrm{T}}(\bar{u}_{i,j} + \bar{u}_{j,i}) \qquad (16)$$

is used, so that after the Z-integration

$$\frac{\partial}{\partial t}\Sigma R^2\Omega + \frac{1}{R}\frac{\partial}{\partial R}\left(\Sigma R^3\left(\Omega\bar{u}_R - \nu_{\mathrm{T}}\frac{\partial \Omega}{\partial R}\right)\right) = \mathcal{L} \qquad (17)$$

results. The magnetic torque is

$$\mathcal{L} = \frac{2R}{\mu_0}\,\bar{B}_Z\,\bar{B}_\phi^{\mathrm{surf}} + \frac{1}{\mu_0 R}\frac{\partial}{\partial R}\left(R^2\int_{-\infty}^{\infty}\bar{B}_R\bar{B}_\phi dZ\right), \qquad (18)$$

where the magnetic fields in the first term of the RHS must be taken at the disk surface. Elimination of the radial inflow velocity from Eqs. (7) and (17) gives the following generalisation of the well-known disk diffusion relation:

$$\frac{\partial \Sigma}{\partial t} + \frac{1}{R}\frac{\partial}{\partial R}\left\{\frac{\mathcal{L} + \frac{1}{R}\frac{\partial}{\partial R}(\nu_{\mathrm{T}}\Sigma R^3\frac{\partial \Omega}{\partial R})}{\frac{1}{R}\frac{\partial}{\partial R}(R^2\Omega)}\right\} = 0. \qquad (19)$$

The magnetic field, however, does not only form large-scale Lorentz forces but it also influences the eddy viscosity in Eq. (19). It is $\nu_{\rm T}$ the Shakura-Sunyaev viscosity $\nu_{\rm T} = \alpha_{\rm SS} H^2 \Omega$ as the reference value.

There is an estimate for (18). If a disk halo with a high conductivity exists, then the surface value of B_ϕ will get large values and the first term in (18) will dominate the magnetic torque $\mathcal{L}$. After Campbell (1992) the shear between the rigidly rotating halo and the accretion disk induces a toroidal magnetic field of

$$\bar{B}_\phi = -\gamma \frac{R}{H} \frac{\rm Pm}{\alpha_{\rm SS}} \frac{\Omega_{\rm K} - \Omega_*}{\Omega_{\rm K}} \bar{B}_Z \tag{20}$$

with Ω_* as the stellar rotation rate (cf. Li et al. 1996). The numerical integration of the induction Eq. (5) for a uniform and a dipolar field confirms this result with the dimensionless parameter $\gamma \simeq 1$ (Figs. 1,2). The toroidal surface field changes its sign at the corotation radius where $\Omega_{\rm K}$ equals the stellar rotation rate Ω_*. The magnetic torque results as negative inside the corotation radius and positive outside the corotation radius. For the steady-state solution of (19) with the viscosity ansatz $\nu_{\rm T} = \alpha_{\rm SS} \Pi / \Sigma\Omega$ one finds for Kepler disks

$$\frac{3\alpha_{\rm SS}}{R} \frac{\partial}{\partial R}(R^2 \Pi) = 2\mathcal{L} + \dot{M}\Omega, \tag{21}$$

where $\dot{M}$ is the integration constant.

Another boundary condition is needed to solve this equation, i.e. $\Pi(R_*) = 0$. Then,

$$\Pi = \frac{2}{3} \frac{\Omega \dot{M}}{\alpha_{\rm SS}} \left(1 - \sqrt{\frac{R_*}{R}}\right) + \frac{2}{3\alpha_{\rm SS} R^2} \int_{R_*}^{R} R\mathcal{L} dR \tag{22}$$

results. Inside the corotation radius, this expression is not positive definite as the last term on its RHS is negative. For a critical amplitude of the vertical magnetic field the expression (22) must become negative so that a disk cannot exist (cf. Miller & Stone 1997). For the magnetic threshold value one simply gets the amplitude

$$\bar{B}_Z \simeq \sqrt{\alpha_{\rm SS} \mu_0 H \Omega \dot{M}} / R \tag{23}$$

resulting in $\bar{B}_Z \simeq \sqrt{10^3 \, \alpha_{\rm SS}}$ Gauss for typical TTS values ($M = 1 M_\odot, \dot{M} = 10^{-7} \, M_\odot/{\rm yr}, R = 6 \cdot 10^{11}$ cm). Note the value as rather low, i.e. only about 3 Gauss for $\alpha_{\rm SS} \simeq 0.01$. The corotation radius normalized with the stellar radius equals $\Omega_*^{-2/3}$ if the stellar rotation Ω_* is normalized with the Kepler rotation of the stellar surface. The corotation radius is thus 4 times the stellar radius if the stellar rotation is only 1/8 of the breakup velocity.

It remains to compute the vertical structure of the disk. To this end the standard procedure can be used. The vertical stratification with inclusion of the magnetic pressure is simply

$$\frac{d}{dZ}\left(p + \frac{\bar{B}_\phi^2}{2\mu_0}\right) = -\rho \Omega_{\rm K}^2 Z, \tag{24}$$

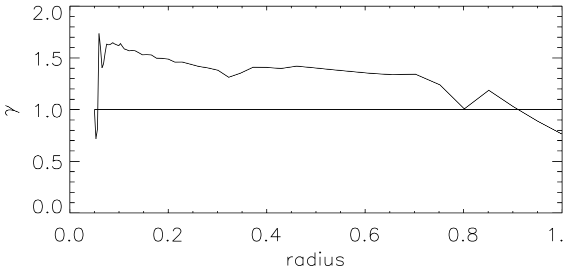

Fig. 1. Uniform external magnetic field: The ratio of the surface toroidal field as the result of the simulation and after (20). The halo is plasma, i.e. its conductivity exceeds the disk conductivity by a factor of 10. We find here $\gamma \simeq 1$

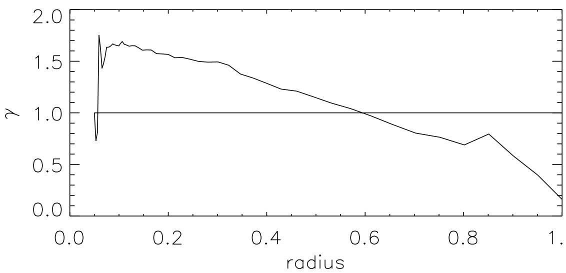

Fig. 2. The same as in Fig. 1 but for a dipolar external magnetic field

by which the disk half-thickness will be defined. Density and pressure are also connected by the polytrope $p = K(r)\rho^\gamma$ where the entropy $K(r)$ shall be defined by its midplane values $K(r) = p_c \rho_c^{-\gamma}$. For $\gamma = 5/3$ and with the standard solution one finds $K \propto \sqrt{R}$.

By comparison of (19) with the mass conservation law (7) the accretion flow $\bar{u}_r$ can be read as $\bar{u}_R = \bar{u}_R^{\rm visc} + \bar{u}_R^{\rm mag}$ with the viscous velocity

$$\bar{u}_R^{\rm visc} = \frac{1}{R\Sigma} \frac{\frac{1}{R}\frac{\partial}{\partial R}(\nu_{\rm T} \Sigma R^3 \frac{\partial \Omega}{\partial R})}{\frac{1}{R}\frac{\partial}{\partial R}(R^2 \Omega)} \tag{25}$$

and the magnetic-driven velocity

$$\bar{u}_R^{\rm mag} = \frac{1}{R\Sigma} \frac{\mathcal{L}}{\frac{1}{R}\frac{\partial}{\partial R}(R^2\Omega)}, \tag{26}$$

which both have to be used in the induction Eq. (5). Various vertical profiles for the radial flow have been applied, among them also the profile derived by Kley & Lin (1992).

3. Results

A standard disk model is used with $\alpha_{\rm SS} = 0.01$ and an inner radius of $3 \cdot 10^{11}$ cm. The stellar rotation approaches 1/8 of the breakup velocity so that the corotation radius in the disk is $12 \cdot 10^{11}$ cm. The outer radius of the disk model is $6 \cdot 10^{12}$ cm. The induction Eq. (5) with (25) and (26) is integrated in time on a 2D domain of the size $0.05 R_{\rm out} < R < R_{\rm out}$ and $-R_{\rm out} < z < R_{\rm out}$ in the system corotating with the central object. In order to get enough grid-points within the disk we used a non-equidistant grid. We fixed the Kepler rotation in the disk and zero-velocity in the corona. The disk structure is

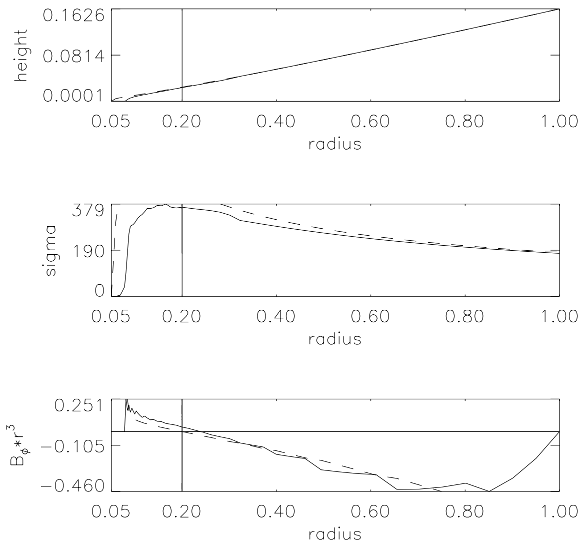

Fig. 3. Disk half-thickness normalized with the outer disk radius, surface density in $\mathrm{g cm^{-2}}$ and toroidal magnetic field amplitude in Gauss (scaled with the normalized radius r^3) for a polar magnetic field of 2 Gauss. The dashed lines show the nonmagnetic solution for both height and surface density as well as the field amplitude after (20). The values of the horizontal axis are normalized with the outer disk radius, the vertical solid line denotes the corotation radius

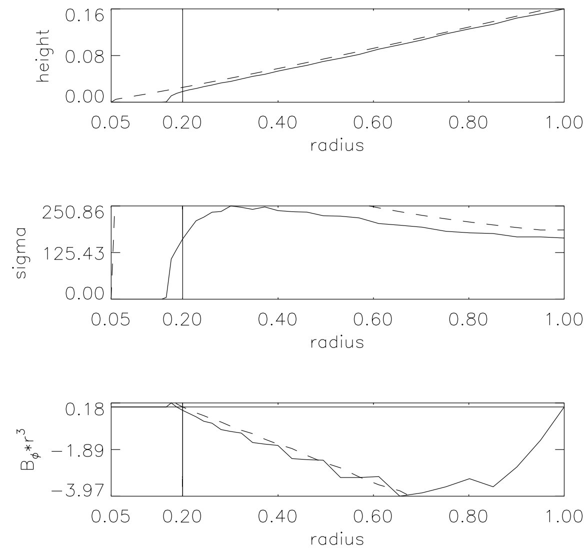

Fig. 4. The same as in Fig. 3 but for 20 Gauss.

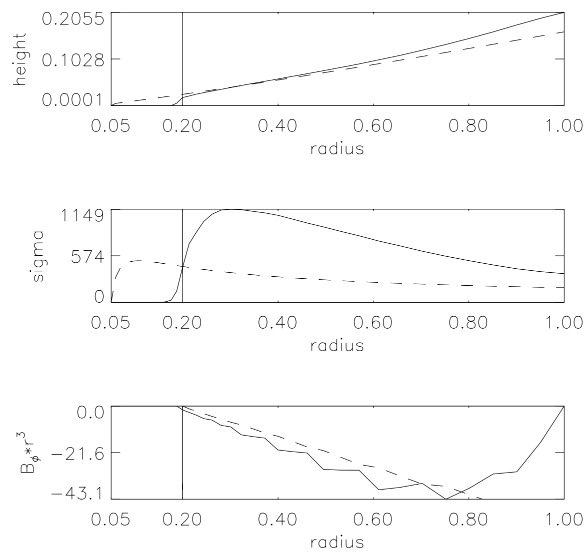

Fig. 5. The same as in Fig. 3 but for 200 Gauss. No disk inside the corotation radius

calculated with the actual magnetic field in the 1+1D approximation from Eq. (19) with (18) and (24) after 10 or 100 time steps, depending on the numerically determined time step of the induction equation. The radial inflow inside the disk is mostly constant in z, because this profile does not really change the results. At the vertical outer boundary of the disk we prescribe the density with the value of the non-magnetic disk in order to calculate the disk height, which is the second time-dependent term in the induction equation. The diffusivity in the corona is the same as in the disk. In order to avoid a negative density during the time evolution, we fix the surface density if it falls below a very small threshold value and set there the disk height to zero. Initially the stellar dipole field penetrates the nonmagnetic α-disk. For weak magnetic fields the disk can partly survive inside the corotation radius. Along this way a disk is provided with both lower surface density and temperature but nearly the same thickness as the nonmagnetic disks (Figs. 3, 4). The solutions become stationary after about 200 outer Kepler orbits. Switching off the magnetic field the disk evolves back to the nonmagnetic solution for all the presented models.

For dipolar fields of about 200 Gauss (at the stellar poles) the disk indeed vanishes inside the corotation radius (Fig. 5). The strong angular momentum extraction from the disk by the magnetic field cannot be balanced by the disk. The time scale for the liquidation of the inner disk with 10 inner rotational orbits is very short. The outer disk is hotter, thicker and more massive than the corresponding nonmagnetic solutions, because of the magnetic driven angular momentum flow from the central object to the outer disk. If no inner disk exists, then the remaining accretion disk favours to spin-down the central object rather than to spin-up.

The same is true for even stronger magnetic fields but in this case the induced toroidal field exhibits the beginning of a saturation. Its amplitude does not longer grow linearly with the vertical field amplitude (Fig. 6). This effect is relevant for the magnetic angular momentum transport in vertical direction, the product of B_ϕ and B_Z seems to get a maximum. The total torque starts with a rather linear relation $\mathcal{L} \propto B^{(0)2}$ while for stronger magnetic fields the relation becomes weaker due to the increasing disk height (Fig. 7). Any spin-down scenario as that of Stępień (1999) for the pre-main-sequence life of Ap-stars has to take into account this effect.

4. Discussion

A thin disk under the influence of a dipolar magnetic field of the central object has been considered. The field is force-free by

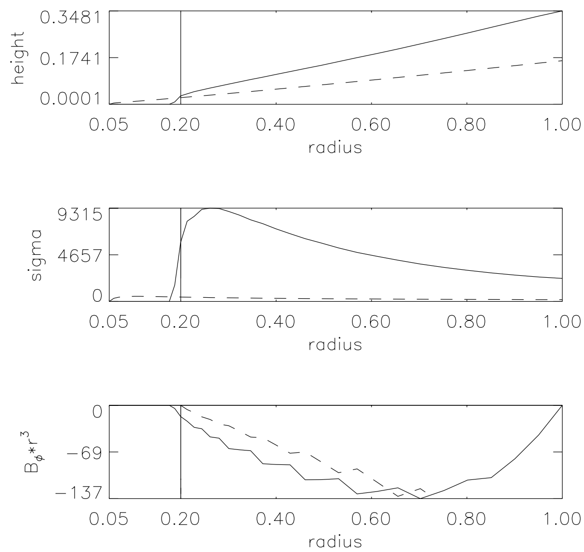

Fig. 6. The same as in Fig. 3 but for 2000 Gauss

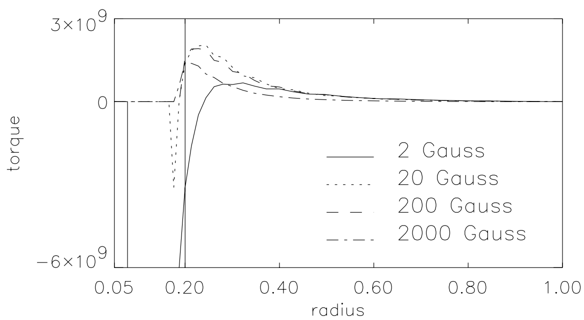

Fig. 7. The magnetic torque (18), normalized with the square of the external magnetic field for various field amplitudes. The magnetic torque inside the corotation radius of the model with 2 Gauss takes its minimum at -10^{12}gs^{-2}. Note the saturation effect for high magnetic amplitudes

definition. Any modification of the disk structure can only be due to the additionally induced magnetic fields. As a result of our simulation with the induction equation for the disk-corona system we find the shear between the differentially rotating disk and the rigidly rotating corona as the main source of induction. All other effects such as the differential rotation of the disk or the accretion flow are negligible. Therefore, an antisymmetric toroidal field is induced which changes its sign at the corotation radius.

The external dipole field is only slightly changed by the radial inflow as already shown by Reyes-Ruiz & Stepinski (1996). This is also the reason why the magnetic field is not expelled from the disk in contrast to the result of Bardou & Heyvaerts (1996). Two forces, i.e. the vertical magnetic pressure gradient and the torque between corona and disk, are able to change the disk structure. The first one tends to decrease the disk thickness. The second one increases (decreases) the accretion flow inside (outside) the corotation radius. For a fixed accretion rate the disk can balance these forces in the stationary regime by decreasing (increasing) its mass inside (outside) the corotation radius. Inside the corotation radius the disks survives only for weak magnetic fields otherwise the density proceeds to zero, and the disk vanishes. The increase of disk mass in the outer part for strong magnetic fields increases also the disk height and the effect of the magnetic pressure becomes negligible in contrast to the result of Liffman & Bardou (1999) where only the magnetic pressure is considered.

The calculations are performed in two dimensions for the induction equation and in the 1+1D approximation for the Navier-Stokes equation in order to exclude all the MHD-instabilities which limit all 2D or 3D simulations to only a few orbit times. With our method we are able to follow the time evolution up to the steady state over thousands of orbits in contrast to the 2D simulation of, e.g., Miller & Stone (1997).

One main assumption for our model is the rigidly rotating corona with its prescribed finite diffusivity. For any increase of the dissipation the radial diffusion would shift the node of the toroidal field outwards beyond the corotation radius. A reduction of the halo dissipation, however, does not change the final stationary solutions.

No prediction can be given with our Z-averaged model about oscillations close to the inner magnetosphere. In addition, the restriction of our model to the stationary-vertical equilibrium does not allow any wind or outflow from the disk towards the corona. Long-term simulations of the disk-halo system are necessary to attack these problems. Further development of the model should include also the energy equation to find the effects of Joule heating for the temperature profile. Only then our preliminary statements about the disk thickness can be improved.

References

André P., Phillips R.B., Lestrade J.-F., Klein K.-L., 1991, ApJ 376, 630
Bardou A., Heyvaerts J., 1996, A&A 307, 1009
Blandford R.D., Payne D.G., 1982, MNRAS 199, 883
Brandenburg A., Campbell C.G., 1998, MNRAS 298, 223
Campbell C.G., 1992, Geophys. Astrophys. Fluid Dyn. 63, 179
Fendt C., Camenzind M., 1996, A&A 313, 591
Ghosh P., Lamb F.K., 1979, ApJ 232, 259
Kley W., Lin D.N.C., 1992, ApJ 397, 600
Königl A., 1989, ApJ 342, 208
Königl A., 1991, ApJ 370, L39
Li J., Wickramasinghe D.T., Rüdiger G., 1996, ApJ 469, 765
Liffman K., Bardou A., 1999, MNRAS 309, 443
Livio M., Pringle J.E., 1992, MNRAS 259, 23
Lubow S.H., Papaloizou J.C.B., Pringle J.E., 1994, MNRAS 267, 235
Miller K.A., Stone J.M., 1997, ApJ 489, 890
Ogilvie G.I., 1997, MNRAS 288, 63
Ogilvie G.I., Livio M., 1998, ApJ 499, 329
Pudritz R.E., 1983, Accretion disk dynamos. In: Soward A.M. (ed.) Stellar and planetary magnetism. Gordon & Breach, New York, p. 223
Reyes-Ruiz M., Stepinski T.F., 1996, ApJ 459, 653
Shalybkov D.A., Rüdiger G., 2000, MNRAS accepted
Stępień K., 1999, A&A submitted